GIANT MOLECULE INTERACTIONS*

S.P. McGLYNN and G.L. FINDLEY

Choppin Chemical Laboratories, Louisiana State University, Baton Rouge, LA 70803 (U.S.A.)

Summary

Molecular Rydberg states are discussed from the point of view of atomic physics, the appropriate molecular extensions being provided where necessary. The interactions of Rydberg states with each other, with intravalence excitations and with their environment are elaborated. A further subdivision is made into channel interactions, strong perturbations and external field effects. By these means it is possible to discuss the molecular Rydberg regime, even at small n, in ways which are remarkably similar to those pertinent to the atom, and hence to generate a coherent picture of the interesting and important area of very large molecules.

1. Introduction

1.1. Pertinence

Giant atoms are currently of considerable concern. Little has been said, however, concerning giant molecules. Both are relevant to the development of future generations of weak field detectors and tunable microwave sensors. In addition, the study of electric and magnetic effects is often inhibited by the inability to generate high field strengths; however, such field effects may be simulated in giant species with relatively small field strengths. Field effect studies are obviously of great concern in astrophysics, plasma physics, photophysics and photochemistry. In photochemistry, for example, electrons are so readily removed from giant systems that novel chemistry must surely result: certain charge transfer to solvent (CTTS) reactions are presumably mediated by such giant states. These states are also of compelling theoretical interest because they demand better formulation of the core–peel separability problem. Finally, the resonance phenomenon, itself a facet of the Rydberg (R) structure, must surely stimulate new approaches both to rate problems and to questions concerning the ability of an N-electron system to support an additional electron (*i.e.* the negative ion problem).

1.2. Scope

The characterization of molecular R transitions is embroiled in decisions concerning the meaning of the term "Rydberg". In atomic physics an R transi-

* Paper presented at the Xth International Conference on Photochemistry, Iraklion, Crete, Greece, September 6 - 12, 1981.

0047-2670/81/0000-0000/$02.50

tion occurs whenever an electron is promoted from a ground state orbital to an upper state orbital possessing an *aufbau* quantum number greater than that of the valence shell. In molecular physics this intuitive clarity is lost in the inability to assign a "principal" quantum number to the valence shell, an inability partially alleviated by heuristic and ambiguous "united atom" arguments.

Alternatively, we may define an R transition as any member of a series which obeys the Rydberg equation

$$E_{j\alpha} = I - \frac{1}{\nu_{j\alpha}^2} \tag{1}$$

where $E_{j\alpha}$ is the energy of that spectral feature thought to be the jth member of the αth R series converging on the ionization limit I and where $\nu_{j\alpha}$ is the effective quantum number. This characterization is empirically limited by the need for spectra which exhibit high resolution over large spectral regions; furthermore, it precludes interactions between R series.

The third alternative is operational: in this case, we say quite simply that an R state is any state defined with respect to an asymptotically hydrogenic hamiltonian. Several conclusions follow.

(i) Energy spacings of R states decrease as $1/\nu_{j\alpha}^2$ where $\nu_{j\alpha} = n_j - \mu_\alpha$ (n_j is an integer and μ_α is the quantum defect).

(ii) The average radius $\langle r \rangle$ of an R orbital is proportional to $\nu_{j\alpha}^2$. Hence, highly excited R states are spatially enormous, a characteristic embodied in the term "giant" molecule or atom.

(iii) For a fixed core the spin–orbit coupling parameter ζ remains approximately constant whereas the exchange integral K decreases at least as fast as $1/\nu_{j\alpha}^2$. Thus, the coupling regime index K/ζ is proportional to $\nu_{j_\alpha}^{-k}$ where $k > 2$, a result indicating that highly excited R states are in a pure (Ω, ω) regime.

We shall adopt the above "asymptotic definition" and then investigate the scope and limitations of the concomitant operational definitions (i) - (iii). In this context we define the following one-electron hamiltonian:

$$H = \frac{\hbar^2}{2m}\left\{-\frac{\mathrm{d}^2}{\mathrm{d}r^2} + \frac{l(l+1)}{r^2}\right\} - \frac{Ze^2}{r} + V_{\mathrm{ra}}(r) + V_{\mathrm{rm}}(r) + V_{\mathrm{so}}(r,\sigma) + \\ + V_{\mathrm{v}}(r,\sigma,Q) + \mathcal{F} \tag{2}$$

The first term in eqn. (2) contains the (radial) kinetic energy operator and the centrifugal barrier, while the second term is the Coulomb potential. V_{ra} is the residual atomic potential and V_{rm} is the residual molecular potential; both of these potentials are short ranged, *i.e.*

$$\lim_{r\to\infty} rV_{\mathrm{ra}} = \lim_{r\to\infty} rV_{\mathrm{rm}} = 0$$

$V_{\mathrm{so}}(r,\sigma)$ represents orbital–orbital and spin–orbital interactions- $V_{\mathrm{v}}(r,\sigma,Q)$ includes vibronic and spin–vibronic interactions. Finally, $\mathcal{F}$ represents any imposed external field, whether electric, magnetic or molecular (*i.e.* condensed phase). This paper represents a justification of eqn. (2) for R states. In Section 2 we present an approximate treatment for V_{ra} and V_{rm} from the viewpoint of single-channel

quantum defect theory (SQDT). In Section 3 we refine this treatment and extend it to include part of V_{so} by the introduction of multichannel quantum defect theory (MQDT) interactions. In Section 4 strong perturbations (*i.e.* those perturbations arising from V_v and from anomalous exchange and spin–orbit coupling effects) are discussed. In addition, the importance and prevalence of Rydberg–valence mixing is investigated. Finally, electric and magnetic field effects are treated in Section 5, while condensed media effects are discussed in Section 6.

2. Single-channel quantum defect theory

2.1. One-electron Coulomb problem

We begin with the hydrogenic atom. The radial Schrödinger equation (in Rydberg units) is

$$\left\{\frac{d^2}{dr^2} - \frac{l(l+1)}{r^2} + \frac{2Z}{r} + 2\mathcal{E}_i\right\} f_i(r) = 0 \tag{3}$$

where

$$\mathcal{E} = -Z^2/k^2 \tag{4}$$

and

$$k = \begin{cases} \nu_i \text{ for } \mathcal{E} < 0 \\ i\gamma \text{ for } \mathcal{E} > 0 \end{cases} \tag{5}$$

The bound state ($\mathcal{E} < 0$) wavefunctions are given by the regular Coulomb function f which asymptotically is

$$f \sim u(\nu, r) \sin \pi\nu - v(\nu, r) \cos \pi\nu \tag{6}$$

where u is a rising exponential and v is a falling exponential in r. Since the bound state wavefunctions must vanish as $r \to \infty$, we find

$$\sin \pi\nu = 0 \tag{7}$$

Thus $\nu = n$ where n is an integer and

$$\mathcal{E} = -Z^2/n^2 \tag{8}$$

2.2. Introduction of the residual atomic potential

The Schrödinger equation for the residual atomic potential is

$$\left\{\frac{d^2}{dr^2} - \frac{l(l+1)}{r^2} + \frac{2Z}{r} - 2V_{ra}(r) + 2\mathcal{E}_{jl}\right\} F_{jl}(r) = 0 \tag{9}$$

Since $V_{ra}(r)$ is short ranged, this equation asymptotically reverts to eqn. (3) at distances greater than r_0, the cut-off distance for V_{ra}. In order to ensure smooth joining at $r = r_0$, we find

$$F_{jl} = f_j(r) \cos \pi\mu_l - g_j(r) \sin \pi\mu_l \tag{10}$$

Using the appropriate asymptotic forms for f and g, eqn. (10) becomes

$$F_{jl} \sim u_j(r) \sin\{\pi(\nu + \mu_l)\} - v_j(r) \cos\{\pi(\nu + \mu_l)\} \tag{11}$$

from which it follows that

$$\sin\{\pi(\nu + \mu_l)\} = 0 \tag{12}$$

or

$$\nu_j = n_j - \mu_l \tag{13}$$

From eqns. (4) and (5) then

$$\mathcal{E}_{jl} = -\frac{Z^2}{(n_j - \mu_l)^2} \tag{14}$$

Thus the Rydberg equation is established.

2.3. Introduction of the residual molecular potential

The procedure of Section 2.2 can be extended to molecules if V_{rm} is indeed short ranged. This in turn implies a significant similarity between an atomic R spectrum and a molecular R spectrum if, in both instances, the *total* residual potential were very nearly the same. That this assumption is reasonable in some cases is established [1] for Xe–CH_3I by a comparison of Figs. 1 and 2.

Further information concerning the residual potentials may be gained through introduction of the phase amplitude method [3]. This *ansatz* transforms the Schrödinger equation into two coupled first-order differential equations, thereby effecting the separation

$$F_{jl}(r) = a_{jl}(r)[f_{jl}(r) \cos\{\pi\mu_l(r)\} - g_{jl}(r) \sin\{\pi\mu_l(r)\}] \tag{15}$$

where $a_{jl}(r)$ is an amplitude function while $\mu_{jl}(r)$ is a quantum defect function. Within the phase amplitude method it is possible to show that

$$\pi\mu_{jl}(r) = 2W^{-1}\int_0^r \{V_{ra}(r') + V_{rm}(r')\}[f_{jl}(r') \cos\{\pi\mu_l(r')\} - g_{jl}(r') \sin\{\pi\mu_l(r')\}]^2 \, dr' \tag{16}$$

where W is the wronskian of the f and g functions.

If the residual potentials are negative and monotonically increasing, it follows from eqn. (16) (and the detailed structure of the f and g functions) that [1]

$$\nu_{jl} - \nu_{(j-1)l} \geqq 1$$

However, if the residual potentials are positive and monotonically decreasing [1]

$$\nu_{jl} - \nu_{(j-1)l} \leqq 1$$

This is illustrated for the rare gases ($V_{rm} = 0$) in Fig. 3. Thus, we see that V_{ra} is attractive for each of the rare gases. Application of this procedure to CH_3I [1]

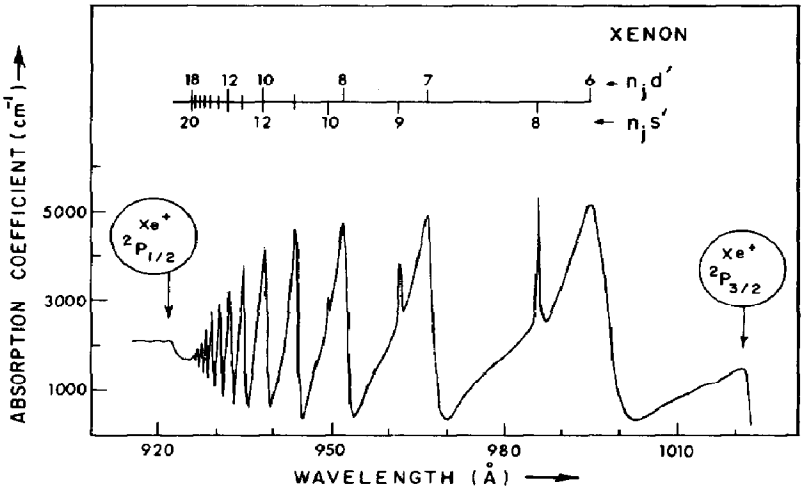

Fig. 1. The autoionization spectrum of xenon between the $^2P_{3/2}$ and $^2P_{1/2}$ ionization limits (adapted from ref. 2). The primed symbol $n_j l'$ distinguishes series converging on $^2P_{1/2}$ from those converging on $^2P_{3/2}$.

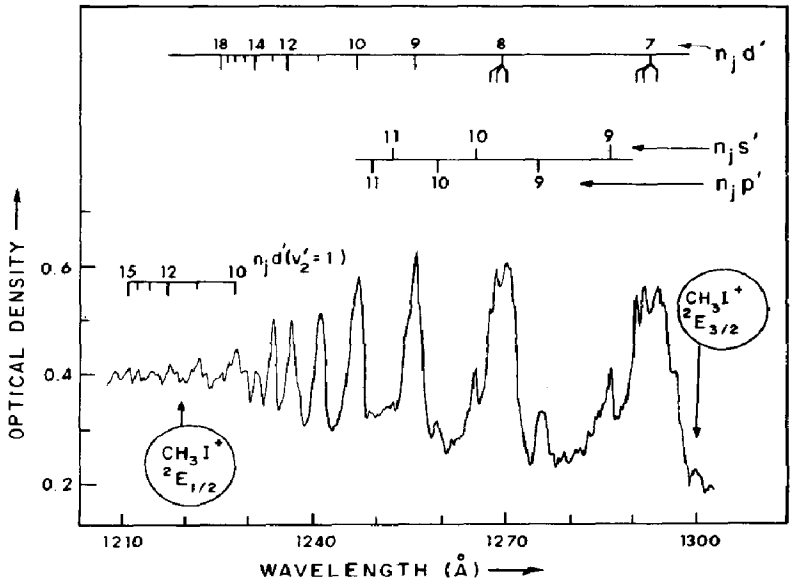

Fig. 2. The absorption spectrum of CH_3I between the $^2E_{3/2}$ and $^2E_{1/2}$ ionization limits. The primed symbol $n_j l'$ distinguishes series converging on $^2E_{1/2}$ from those converging on $^2E_{3/2}$.

shows that V_{rm} is repulsive for $j < 2$ but becomes negligible at larger j because of the dominance of $V_{ra}(r)$ at larger r. The effect is even more pronounced for l waves with $l \geqq 2$ since, in this case, the centrifugal barrier acts to impose effective spherical symmetry even on the molecular system [1].

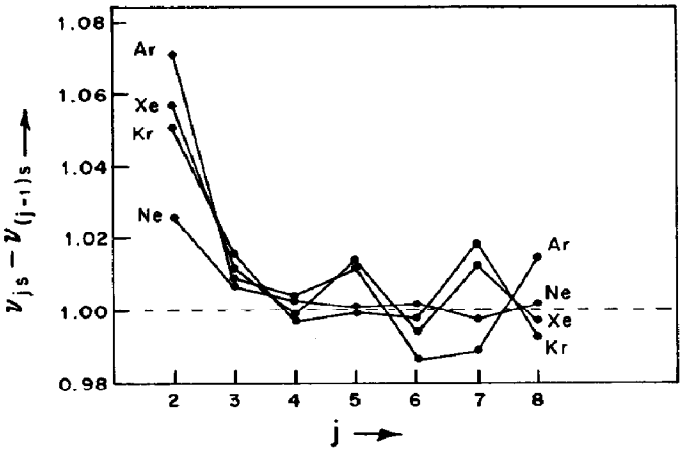

Fig. 3. A plot of $\nu_{js} - \nu_{(j-1)s}$ for the $n_0p^6\ {}^1S_0 \rightarrow n_0p^5 n_j s_{3/2}{}^0, J = 1$ series ($^2P_{3/2}$ core) of the rare gases (data taken from ref. 4).

3. Multichannel quantum defect theory

If two or more ionization limits are adjacent, two R series (one converging on each limit) may interact, presuming, of course, that each series has the same total angular momentum [5]. Of even more importance, a discrete state of one series may interact with the continuum of the other series thereby preionizing (autoionizing). A "channel" is the union of the discrete members of an R series with the continuum of the same series, and interactions such as those described above are known as multichannel interactions. That such interactions occur in xenon [6] and CH_3I [1, 7] is shown in Figs. 1 and 2: we see the characteristic Beutler–Fano [8 - 10] autoionization profiles in both systems. Within the MQDT, however, the similarities between xenon and CH_3I can be further strengthened [11], as will now be shown.

In the spectral region of interest in xenon and CH_3I there are two ionization limits: $I_1 = I(^2P_{3/2}$ or $^2E_{3/2})$ and $I_2 = I(^2P_{1/2}$ or $^2E_{1/2})$. Thus each level must be referenced to both ionization limits:

$$E = I_1 - \frac{I}{\nu_1{}^2} = I_2 - \frac{1}{\nu_2{}^2} \tag{17}$$

Boundary conditions on the bound state wavefunctions impose a consistency constraint which, when coupled with eqn. (17), allows us to fit experimental data to a ν_1(modulo 1) *versus* ν_2(modulo 2) plot and thus to determine quantum defects [6, 10, 12]. This procedure is illustrated in Fig. 4. The similarities between the two plots are striking and further indicate the close relationship of the non-coulombic potential terms for xenon and CH_3I.

Finally, we note that manifestations of autoionization in polyatomic systems are known [13] which are more esoteric (*e.g.* J dependence and q reversal) than that discussed above. In addition, rotational and vibrational preionization and molecular predissociation have been treated in an MQDT format [10, 14 - 16].

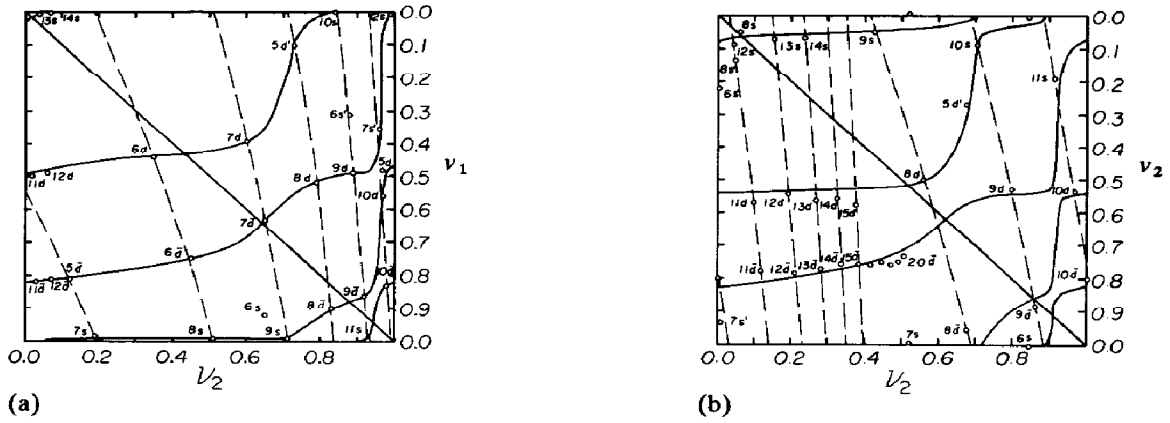

Fig. 4. Lu–Fano [6, 10, 12] plots for the discrete states of (a) xenon and (b) CH_3I. The xenon plot is adapted from ref. 6. ν_1 and ν_2 are effective quantum numbers (modulo 1) defined with respect to the first and second ionization potentials respectively (see text). The full diagonal lines are given by $\nu_1 = \nu_2$; the broken curves are plots of $\nu_2(\nu_1)$, the functionality being defined by eqn. (17) of the text. The full curves are the loci of the consistency constraint mentioned in the text and discussed more fully in refs. 6 and 11. The data point notation is as follows: $d = d_{5/2}(I_1)$; $\bar{d} = d_{3/2}(I_1)$; $s = s_{1/2}(I_1)$; $s' = s_{1/2}(I_2)$; $d' = d_{3/2}(I_2)$.

4. Strong perturbations

Most, if not all, of the strong perturbations considered here should be included within the channel framework of Section 3. Unfortunately, the theoretical basis for such an inclusion is not available for polyatomics and is even incomplete for diatomics [10, 14 - 16]. Indeed, even if the tactical approach were fully developed, considerations of the multichannel nature would require detailed high resolution data over large spectral ranges. Such data, unfortunately, are not often available.

The general type of high resolution data covers small spectroscopic ranges (*e.g.* the first s complex of CH_3I [17]) and perturbations may be evident which, because of the narrow observational range, require discussion in terms of interactions within that range. Even in the MQDT, sudden perturbations may occur which, because of artificial restrictions on the number of interacting channels, simply cannot be treated within the channel framework. The above two types of perturbations are referred to here as strong perturbations not because they are strong but because they are (or appear to be) sudden and therefore in some sense dominating.

As a result we now feel free to discuss a variety of strong perturbations of which at least one (*i.e.* spin–orbit coupling) has already been considered within the MQDT.

4.1. Spin–orbit coupling

We use the 5p → 6s R excitation of HI as an example. It is found that the linear ≡C–I bond of alkyl, alkene and alkyne iodides dominates spin–orbit cou-

pling in these iodides and therefore that the HI considerations have a wider range of applicability than we might at first think. Indeed, because the spin–orbit coupling constants for chlorine, bromine or iodine are all much larger than that for carbon, these same considerations also apply to chlorides and bromides.

The states which arise from the 5p → 6s configurational excitation are shown in Fig. 5 in both the (Λ,S) limit and the (Ω,ω) limit. If the states shown in Fig. 5 are labelled 1, 2, 3 and 4 in order of increasing energy, then the intermediate coupling regime yields the following set [18] of energy differences and intensity ratios:

$$E(4)-E(2) = 2(K^2+\zeta^2)^{1/2}$$

$$E(3)-E(1) = 2\zeta$$

$$E(2)-E(1) = K-(K^2+\zeta^2)^{1/2}+\zeta$$

$$E(4)-E(3) = K+(K^2+\zeta^2)^{1/2}-\zeta$$

$$I(^2\Pi_{3/2})-I(^2\Pi_{1/2}) = 2\zeta$$

$$\frac{\mathcal{J}(4)}{\mathcal{J}(2)} = \left\{\frac{K}{\zeta}+\left(1+\frac{K^2}{\zeta^2}\right)^{1/2}\right\}^2$$

Here K is the exchange integral, ζ is the spin–orbit coupling constant ($K \equiv \langle 5p6s|\,1/r_{12}\,|6s5p\rangle$ and $\zeta \equiv \frac{1}{2}\langle 5p|\,\zeta\,|5p\rangle$) and $\mathcal{J}(\beta)$ is the absorptivity of the transition $\tilde{X} \rightarrow \beta$. The ability of this model in fitting details of intermediate coupling in the simple halides is extensive [19, 20], as may be seen in Fig. 6.

4.2. *Vibronic and spin–vibronic coupling*

If q, Q and σ represent sets of electron coordinates, atom coordinates and electron spin coordinates respectively, the spin–vibronic hamiltonian may be designated $H(q, \sigma, Q)$. If we assume that spin–orbit coupling is small, a Herzberg–Teller expansion in the normal coordinates Q_K about the equilibrium nuclear configuration Q° of a given electronic state yields

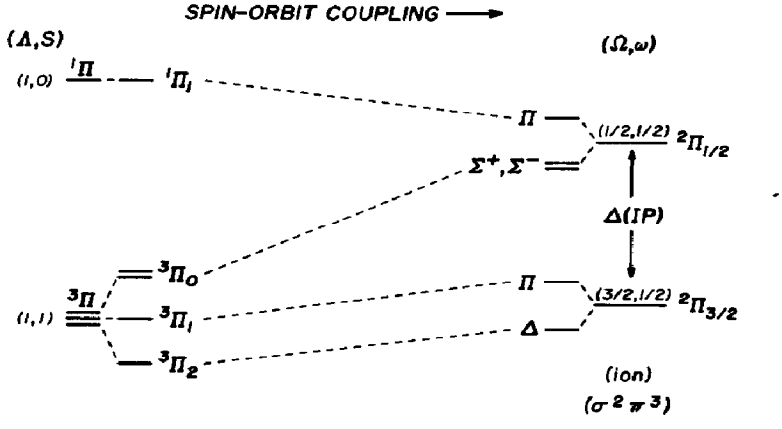

Fig. 5. Spin–orbit coupling in the $...\sigma^2\pi^3 6s$ configuration of HI.

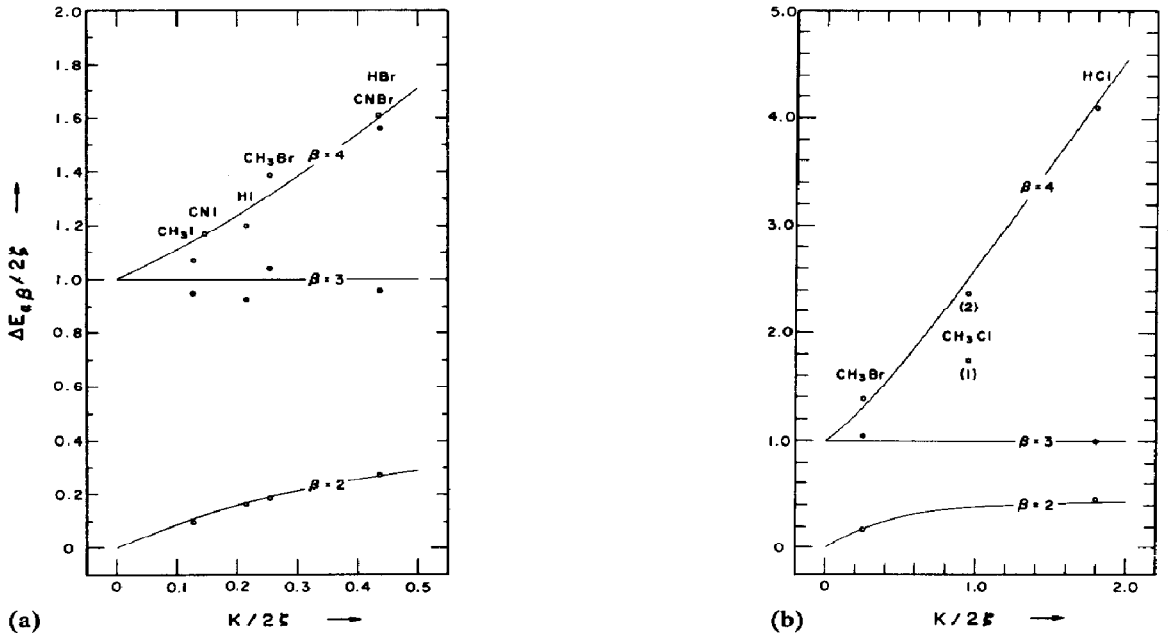

Fig. 6. A plot of $\Delta E_{\alpha\beta}$, $\alpha = 1$ and $\beta = 2, 3, 4$, *vs.* the exchange:spin–orbit ratio for various halides: ——, theoretical curves (see Section 4.1); ○, ●, experimental data.

$$H(q, \sigma, Q) = H(q; Q^\circ) + H(q, \sigma; Q^\circ) + \sum_k \left[\left\{ \frac{\delta H(q, Q)}{\delta Q_K} \right\}_{Q^\circ} + \left\{ \frac{\delta H(q, \sigma, Q)}{\delta Q_K} \right\}_{Q^\circ} \right] Q_K + \ldots \tag{18}$$

which, on truncation, may be written

$$H(q, \sigma, Q) = H_e + H_{so} + H_v + H_{sv} \tag{19}$$

where H_e is the Born–Oppenheimer electronic hamiltonian at configuration Q°, H_{so} is the spin–orbit hamiltonian (also at Q°), H_v and H_{sv} (in obvious notations) are the vibronic and spin–vibronic hamiltonians and all coordinate dependences to the right of the semicolon are parametric. If the H_e–H_{so} separation is valid, then $H_{so} < H_e$ and hence H_v and H_{sv} respectively are first and second order in nature. If H_{so} is large, it is advisable to rewrite eqn. (18) as

$$H(q, \sigma, Q) = H(q, \sigma; Q^\circ) + \sum_k \{\delta H(q, \sigma, Q)\, \delta Q_K\}_{Q^\circ} Q_K \tag{20}$$

in which case H_{sv}, now the second term, is formally first order.

In the MQDT, as presented in Section 3, the zeroth-order electronic and spin–orbit interactions are included in the channel formalism and they need not be considered here. However, the vibronic and spin–vibronic interactions are

TABLE 1

State	$\{q_i\}$	$\{q_i,\sigma_j\}$	$\{q_i,\sigma_j,Q_{1,2,3}\}$	$\{q_i,\sigma_j,Q_{4,5,6}\}$
1	Π	Δ	Δ	Φ,Π
2	Π	Π	Π	Π,Σ^+,Σ^-
3	Π	Σ^+,Σ^-	Σ^+,Σ^-	Π
4	Π	Π	Π	Π,Σ^+,Σ^-

not a part of the MQDT, at least as we have formalized it. Hence these effects can give rise to spectroscopic perturbations which are not only *not* accounted for within the MQDT but which can also confuse the entire MQDT deperturbational tactic. Thus it is very important to recognize vibronic and spin–vibronic intrusions, particularly because these intrusions are both common and large.

We again adopt the linear HI molecule as an exemplar of vibronic and spin–vibronic coupling. This molecule possesses only one normal vibrational mode, which forms a basis for the Σ^+ representation of $C_{\infty v}$. The extension to the CH_3I molecule is accomplished here, for simplicity, by "permitting" HI to possess non-totally symmetric Π normal modes. Thus in the group $C_{\infty v}$ the CH_3I normal modes Q_1, Q_2 and $Q_3 \in \Sigma^+$ and Q_4, Q_5 and $Q_6 \in \Pi$. Consequently, we are now in a position to tabulate the representations of $C_{\infty v}$ for which the various vector collections form bases (Table 1).

Now, in the (Λ,S) regime (Table 1, second column) only the $\tilde{X} \rightarrow 4$ transition, namely $^1\Sigma^+ \rightarrow {}^1\Pi$, is electric dipole allowed. In the (Ω,ω) regime (Table 1, third column), spin–orbit mixing of states 2 and 4 confers allowedness the $\tilde{X} \rightarrow 2$ transition. The transitions $\tilde{X} \rightarrow 1$ and $\tilde{X} \rightarrow 3$, however, remain forbidden and retain this forbiddenness until vibronically coupled to either state 2 or state 4 by Π normal modes (Table 1, fifth column). We thus have the interesting result that states 2 and 4 may be coupled in a nominally first-order way by totally symmetric modes, whereas states 1 and 3 can couple with either of states 2 and 4 in ways which are nominally second order, and that such coupling is mediated only by non-totally symmetric modes. An example [21] of 3–4 state coupling in CD_3I mediated by the Q_6 mode is shown in Fig. 7. Examples [22] of 2–4 mixing abound. The matrix elements of the nominally first-order and second-order effects are as follows: C_2H_5Br [22] (2–4 mixing), 145 cm^{-1}; CNCl [23] (4–intravalence mixing), 180 cm^{-1}; CH_3I [21] (3–4 mixing), 15 cm^{-1}.

5. Field effects

5.1. Magnetic field effects

The application of a magnetic field B introduces the Zeeman term $H_B = \mu \cdot B$ (where μ is the magnetic moment) into the hamiltonian. Given the normal bandwidths for polyatomic molecules, it is improbable that line splitting due to the Zeeman effect will be observed in such systems, at least for $B \leqq 20$ T. The observation of Zeeman effects then devolves on the measurement of band shape differences, *e.g.* the measurement of magnetic circular dichroism (MCD) [24],

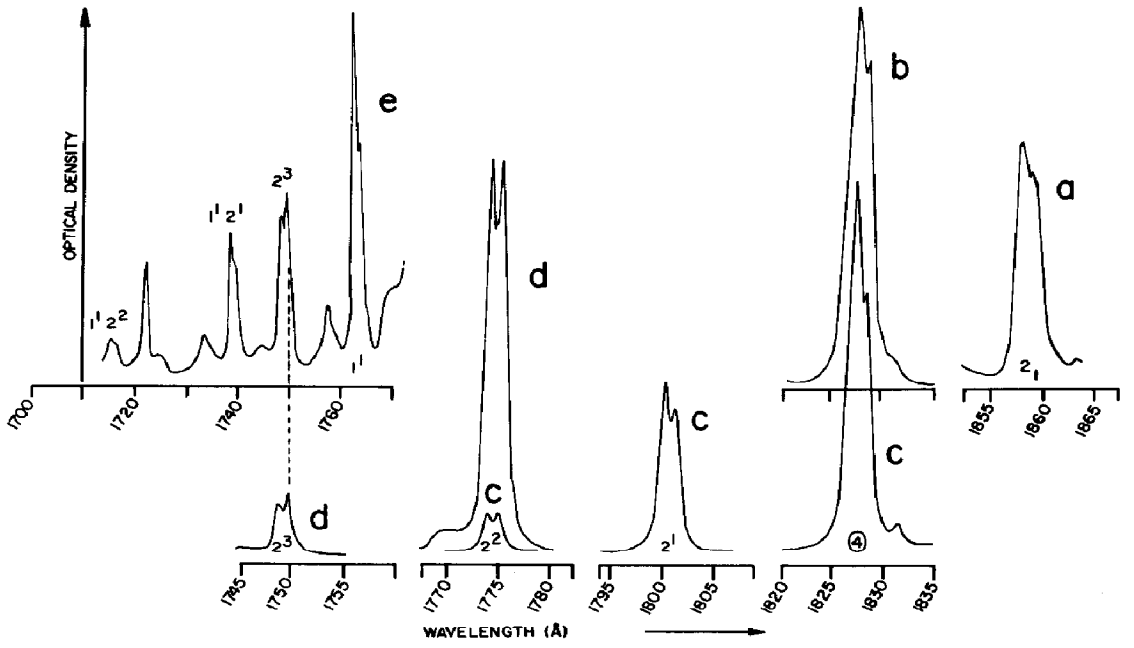

Fig. 7. Spin–vibronic doubling in CD_3I mediated by the non-totally symmetric (Π symmetry) mode Q_6. The interactions in this case occur between states $0 \rightarrow 3$ (ν_6) and states $0 \rightarrow 4$ and are carried throughout the ν_2 progression of Q_2 built on the transition $0 \rightarrow 4$. The alternation in intensity is associated with a slight difference in the frequency ν_2 in states 3 and 4. The doubling is absent in CH_3I because the increase in the ν_6 frequency in the fully protonated derivative destroys the near degeneracy.

which is the difference in molecular absorptivity of left and right circularly polarized light in the presence of a magnetic field. The primary aim of such studies is to make state assignments. Unfortunately, difficulties intrude. For example, μ is different in the various molecular spin–orbit limits of which, in contrast with the atom, there are more than two (*i.e.* (Λ,S) and (Ω,ω)). Indeed, the only well-defined quantum number is a resultant of molecular rotational and electronic motions. The situation, then, is very complicated in a diatomic molecule; in a polyatomic molecule, because of large coriolis effects it can become even worse.

It has been shown [20, 25], however, that MCD can lead to rather precise information. We exemplify again using the first s complex of CH_3I in a primitive $C_{\infty v}$ point group. In this instance we find the spectra shown in Figs. 8 and 9 [25]. The MCD signal is [25]

$$\Delta A^{H}(\bar{\nu}_0) = A^{H}_{-}(\bar{\nu}_0) - A^{H}_{+}(\bar{\nu}_0) = aB \left\{ \frac{\delta A^{0}(\bar{\nu})}{\delta \bar{\nu}} \right\}_{\bar{\nu}_0} + bBA^{0}(\bar{\nu}_0) \qquad (21)$$

where A denotes absorptivity, the superscripts H and 0 denote the presence or absence of the field B and the subscripts + and – denote right circularly polarized light and left circularly polarized light respectively. Since the ground state $^1\Sigma^+$ possesses no angular momentum and therefore a is proportional to μ_β of the

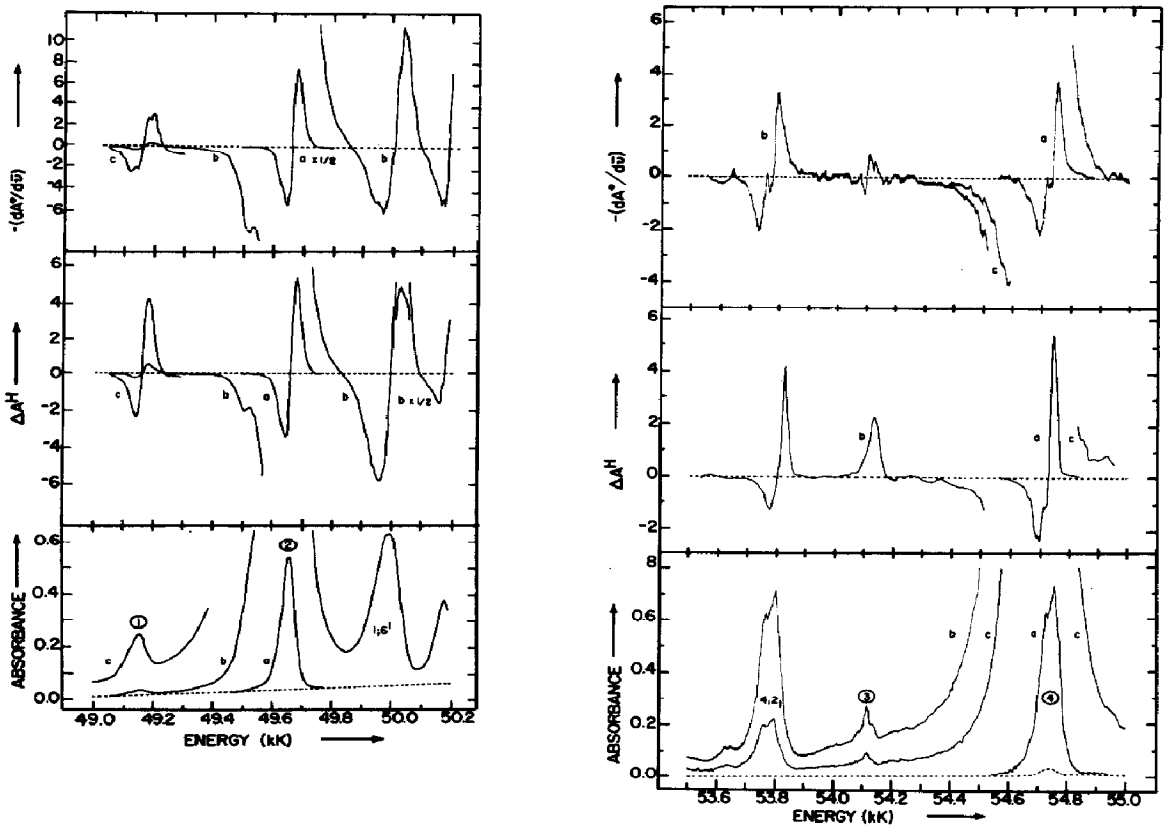

Fig. 8. Absorption spectra A^0, MCD spectra ΔA^H and derivative spectra $dA^0/d\bar{\nu}$ of CH_3I in the 6s Rydberg complex.

Fig. 9. Absorption spectra A^0, MCD spectra ΔA^H and derivative spectra $dA^0/d\bar{\nu}$ of CD_3I in the 6s Rydberg complex.

excited state β, the derivative component of eqn. (21) will be large when μ_β is large and absent when μ_β is zero. The second term in eqn. (21), attributable to field-induced mixing, is usually small and will only be important when a is zero. The relevant factors are that a derivative signal (+ or – phase) denotes an excited state magnetic moment whose size, $\mu_\beta = -(\Lambda_c + 2\Sigma_c + \lambda + 2\sigma)\hbar^{-1}\mu_{Bohr}$ in (Ω,ω) coupling, is proportional to signal height and that an absorptive-type signal (+ or – phase) denotes an excited state with zero magnetic moment.

The experimental magnetic moments of states 1, 2, 3 and 4, as evaluated [25] from the data of Figs. 8 and 9, are 1, 0.33, 0 and 0.27, whereas those obtained using the μ_β expression given above are 1, 0.33, 0 and 0.33, in excellent agreement with experiment. A great deal of other information is contained in the phasing and is discussed in refs. 25 and 26.

The quadratic field effect, attributable to diamagnetism, is usually very small. However, since the diamagnetic interactions are proportional to the Rydberg cross-sectional area, they increase as ν^4 whereas the electrostatic binding energies decrease as ν^{-2}. Thus the ratio of magnetic energy to electrostatic bind-

ing energy increases as ν^6 and at $n = 30$, for example, is about 10^9 times larger than for $n = 1$. In this case the quadratic field effect not only dominates the Zeeman effect but also overwhelms the electrostatic binding energy and converts the system into a "magnetic system". Quadratic field effects have been observed in atoms [27, 28] and although a thorough understanding is elusive it appears to be nascent. We [29] have searched CH_3I and C_6H_6 for quadratic field effects in the vicinities of both I_1 and I_2. Although distinct field perturbations were evident [29], no behavior reminiscent of a magnetic system was observed. The doublet intensification observed [29] at $n = 15$ in CH_3I is probably a $|\Delta J| = 2$ field-induced mixing of the s–d type.

5.2. Electric field effects

The investigation of molecules in strong external electric fields, while burgeoning [30], is still in its infancy. The goad for research is provided by the development of focused pulsed laser systems with power densities in the gigawatts per square centimeter range which are strong enough to produce massive distortions of molecular electronic charge distributions. The Rydberg regime provides a facile means of performing such "high field" investigations. Since the mean Coulomb field of a Rydberg molecule is $eZ/\langle r^2 \rangle \propto \nu^{-4}$ it follows that even a very weak field can induce field ionization at large n values. Furthermore, since level densities increase as ν^5, it follows that weak-field-induced mixings and hence massive non-linearities can occur in high n Rydberg states. Unfortunately, few or no investigations of high n molecular states are known. Indeed, the little vacuum UV work known [24, 31, 32] is mostly concerned with state identifications.

The electron of a hydrogenic system in a static electric field finds itself in the potential

$$V(r) = -\frac{Z}{r} + \boldsymbol{E} \cdot \boldsymbol{r} \tag{22}$$

The effect of the term $H_E = \boldsymbol{E} \cdot \boldsymbol{r}$ is to couple the discrete states of the field-free atom, producing changes in the atom structure (*i.e.* Stark effects). However, it can also produce discrete state–continuum coupling, leading to field ionization and to a real alteration in the ionization limit. The situation in a molecule is very different from that in the atom: the molecule possesses dipole moments, different in both ground (unprimed) and excited (primed) states, which the atom does not. Thus, if we define $\boldsymbol{a} = \boldsymbol{\mu} - \boldsymbol{\mu}'$, asserting that both dipole moments are either parallel or antiparallel to the principal molecular axis (which itself lies at an angle ϑ to $\boldsymbol{E}$) and if we define $b = \alpha - \alpha'$ where α is a mean isotropic polarizability, we can write [31]

$$H_E(\vartheta) = \frac{\boldsymbol{a} \cdot \boldsymbol{E}}{hc} - \frac{bE^2}{2} \tag{23}$$

The total effects are considerably more complex than that implied above. Yet, as far as we are concerned, eqn. (23) contains the essence of our interests. Thus the Stark effect measurements (low n or low field) provide a way of measuring μ', and the effect of measurements at high n, quadratic because α' varies as ν^6, will yield a measure of α'.

Again, because of bandwidth problems, the measurement of molecular Stark effects usually devolves on the detection of band shape alterations. An applicable method has been discussed [24] and a few examples [31, 32] of its use are available. Briefly, the experimental format known as electric linear dichroism is preferable. If the electric vector ε of the incident light wave is plane polarized and at an angle β to the external electric field E (which in turn is perpendicular to the direction of light incidence), the field-on–field-off absorbance difference is [24]

$$\Delta A^{E}_{\beta}(\bar{\nu}_0) \equiv A^{E}_{\beta}(\bar{\nu}_0) - A^{0}(\bar{\nu}_0)$$

$$= E^2\left(C_1^{\beta}A^0(\bar{\nu}_0) + C_2^{\beta}\left[\left\{\frac{dA^0(\bar{\nu})}{d\bar{\nu}}\right\}_{\bar{\nu}_0} - \frac{A^0(\bar{\nu}_0)}{\bar{\nu}_0} + \right.\right.$$

$$\left.\left. + C_3^{\beta}\left[\left\{\frac{d^2A^0(\bar{\nu})}{d\bar{\nu}^2}\right\}_{\bar{\nu}_0} - \frac{2}{\bar{\nu}_0}\left\{\frac{dA^0(\bar{\nu})}{d\bar{\nu}}\right\}_{\bar{\nu}_0} + \frac{2A^0(\bar{\nu}_0)}{\bar{\nu}_0^2}\right]\right) \qquad (24)$$

This expression is obviously more complex than that in the magnetic field case primarily because of the presence of the second derivative. Expressions for the parameters C_1, C_2 and C_3 are available [24] in terms of dipole moments, polarizability tensor components and field-induced mixing coefficients, and experimental means of extracting them are known.

6. Rydberg series in the condensed phase

It is impossible to discuss molecular R series in solution without an understanding of them in the gas phase. Unfortunately, our understanding of gas phase behavior is not very good and for that reason we feel compelled to initiate our discussion of the condensed phase by a retreat to the gaseous phase.

6.1. Gas phase

In the vapor, molecules may exhibit the following characteristics: (i) a well-developed R series, almost hydrogen like in that the intensity decreases as $1/\nu^3$; (ii) a well-developed R series but with maximum intensity at intermediate values of n; (iii) a collapsed R series, often with only the lowest energy member observable (*e.g.* the lowest R (s) transitions in H_2O, amides, saturated hydrocarbons etc. which may be referred to, facetiously perhaps, as "virgin Rydbergs", characterized usually by being anomalously broad, intense and quantum defect deviant [33]); (iv) a series such as (i) or (ii) but with an anomalous quantum defect for the first few members [34] (see, for example, our discussion of SQDT).

Rydberg series may, of course, exhibit many perturbations, the recognition and identification of which has been the content of Sections 3 and 4. Now we concern ourselves primarily with the series characteristics (i) - (iv). It seems to us that the only model capable of rationalizing items (ii) - (iv) is a double-well model (Fig. 10).

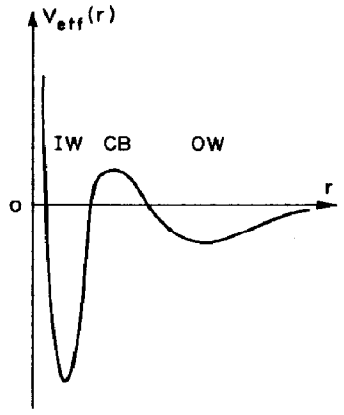

Fig. 10. A model double-well potential: IW, inner well; CB, centrifugal barrier; OW, outer well.

For atomic Rs, $V(r)$ is a monotonically increasing negative-definite function of r. However, the effective potential

$$V_{\text{eff}}(r) = V(r) + \frac{l(l+1)}{r^2}$$

is monotonic only for s waves. For l waves, $l \neq 0$, $V_{\text{eff}}(r)$ is generally double welled and exhibits a centrifugal barrier such that the bound states may be approximate eigenstates of either the inner well (IW) or the outer well (OW). The barrier controls the finite number of bound states, some perhaps resonant, which can be sustained in the IW. The OW potential is asymptotically hydrogenic and it sustains an infinite number of R states.

For molecular Rs, since $V_{\text{rm}}(r)$ is short ranged, the effective potential is essentially spherically symmetric at large r. At small r, however, the effects of $V_{\text{rm}}(r)$ are drastic. From an atomic point of view the imposition of $V_{\text{rm}}(r)$ on an atomic potential is a breaking of symmetry of the sphere group. Retaining $V_{\text{eff}}(r) = V_{\text{eff}}(r)$, the result is the induction of l wave mixing in a spherically symmetric potential. Thus, even for a parental s wave, the effective potential for a molecule will be of the double-well form but the barrier may be negative definite: $V_{\text{eff}}(r)$ may be a double-well potential for molecular R states regardless of the parental l value. As for atoms, the nature of the barrier determines the number of bound levels in the IW and, more importantly, the localization of wave amplitude in either the IW or the OW regions.

We now attempt to rationalize the gas phase characteristics. In order to do so, we note that the initiating orbital in the absorptive event is largely confined in the IW and, consequently, that only those terminal R orbitals with some IW amplitude will couple optically to the ground state. In this view, then, rationalization proceeds as follows: (i) the centrifugal barrier (CB) is either very weak or absent; (ii) the barrier is weak and narrow and, while the IW cannot sustain even one bound level, all levels are bimodal (*i.e.* possess IW and OW amplitude) and the bimodal IW component maximizes at intermediate n; (iii) one or more levels can be sustained in the IW, the barrier being such that all eigenfunctions

are either wholly IW or wholly OW and that little bimodality (*i.e.* mixing) occurs; (iv) there is always a bimodal component in the first s R member.

6.2. Condensed phase

Consider now a molecule-doped insulator, liquid or solid. The dopant molecules exhibit the following behavior forming the condensed phase: (v) virgin R states (see (iii) above) remain largely unaffected [33]; (vi) total quenching of R series (see (i) above) is common [34, 35]; (vii) a Wannier exciton behavior results and a few members of the exciton R series are observed in some instances [36]; (viii) anions which do not support any bound excited states in the gas phase may do so in the condensed phase (some of these states may be resonant and may lead to electron transfer (*i.e.* CTTS [37]) phenomena in aqueous solutions and single-crystal hosts [33]).

The alterations in $V_{\text{eff}}(r)$ caused by condensation of the guest into a condensed insulator host are as follows. To first order, $V_{\text{eff}}(r)$ remains unaffected by the crystal field of the host at small r; at large r the conduction band of the host will dominate $V_{\text{eff}}(r)$ so that

$$\lim_{r\to\infty} I(\text{dopant}) = E(\text{conduction band})$$

and at intermediate r further substructure (*i.e.* negative-definite barriers) may or may not appear in the OW region. If the dopant is a charged entity such as an anion, the resulting host–guest interactions become so drastic that even the IW region is grossly altered [38]. Indeed, in this case the deepening of the IW may support bound states and, if substructure appears in the intermediate r region, some of these states may become resonant (*i.e.* may autoionize to the host conduction band). The behavioral characteristics (v) - (viii), then, are rationalized as follows: (v) these states, already localized in the IW, remain largely unaffected by the environment; (vi) the host conduction band must lie near or below the first R series member and $V_{\text{eff}}(r)$ substructure in the OW region must be minimal; (vii) the host conduction band must lie above the first few R series members and/or a large substructure of $V_{\text{eff}}(r)$ must occur in the OW region; (viii) the events already discussed for a monopolar dopant must occur.

7. Conclusions

We have tried to assess the Rydberg area of molecular electronic structure and interactions in the frame of modern atomic physics, building on the appropriate molecular extensions where needed. In the course of this effort it became totally obvious that the chemical literature is not only *not* keeping pace with the rapidly advancing area of atomic physics but that it is also losing ground in molecular physics. We believe this to be most unfortunate because it puts the chemist at a distance from the cutting edge of his subject. As examples we note that progress in high energy chemistry is tied in a large measure to our understanding of R states; rare gas chemistry, a rather startling discovery in the first place, may well rely heavily on Feschbach resonances, and much preparative chemistry may well require CTTS intermediates.

Acknowledgment

This work was supported by the U.S. Department of Energy.

References

1 H.-T. Wang, W.S. Felps, G.L. Findley, A.R.P. Rau and S.P. McGlynn, *J. Chem. Phys., 67* (1977) 3940.
2 R.G. Huffman, Y. Tanaka and J.C. Larrabee, *J. Chem. Phys., 39* (1963) 902.
3 J.L. Dehmer and U. Fano, *Phys. Rev. A, 2* (1970) 304.
4 C.E. Moore, *Natl. Bur. Stand. Circ. 467,* 1958 (U.S. Government Printing Office, Washington, DC).
5 M.J. Seaton, *Proc. Phys. Soc., 88* (1966) 801, 815.
6 K.T. Lu, *Phys. Rev. A, 4* (1971) 579.
7 M.A. Baig, J.P. Connerade, J. Dagata and S.P. McGlynn, *J. Phys. B, 14* (1981) L25.
8 H. Beutler, *Z. Phys., 93* (1935) 177.
9 U. Fano, *Phys. Rev., 124* (1961) 1866.
10 U. Fano, *Phys. Rev. A, 2* (1970) 353.
11 J. Dagata, G.L. Findley, S.P. McGlynn, J.P. Connerade and M.A. Baig, submitted to *Phys. Rev. A.*
12 K.T. Lu and U. Fano, *Phys. Rev. A, 2* (1970) 81.
13 J.P. Connerade, M.A. Baig and S.P. McGlynn, *J. Phys. B, 14* (1981) L67.
14 O. Atabek and C. Jungen, in H. Kleinpoppen and M.R.C. McDowell (eds.), *Electron and Photon Interactions with Atoms,* Plenum, New York, 1976.
15 D. Dill and Ch. Jungen, *J. Phys. Chem., 84* (1980) 2116.
16 Ch. Jungen and D. Dill, *J. Chem. Phys., 73* (1980) 3338.
17 S. Felps, P. Hochmann, P. Brint and S.P. McGlynn, *J. Mol. Spectrosc., 59* (1976) 355.
18 R.S. Mulliken, *Phys. Rev., 57* (1940) 500.
19 W.S. Felps, G.L. Findley and S.P. McGlynn, *Chem. Phys. Lett.,* in the press.
20 S.P. McGlynn, J.D. Scott, W.S. Felps and G.L. Findley, *J. Chem. Phys., 72* (1980) 421.
21 S.P. McGlynn, W.S. Felps, J.D. Scott and G.L. Findley, *J. Chem. Phys., 73* (1980) 4925.
22 W.S. Felps, J.D. Scott, G.L. Findley and S.P. McGlynn, *J. Chem. Phys., 74* (1981) 4832.
23 W.S. Felps, S.P. McGlynn and G.L. Findley, *J. Mol. Spectrosc., 86* (1981) 71.
24 J.D. Scott, W.S. Felps and S.P. McGlynn, *Nucl. Instrum. Methods, 152* (1978) 231.
25 J.D. Scott, W.S. Felps, G.L. Findley and S.P. McGlynn, *J. Chem. Phys., 68* (1978) 4678.
26 J.D. Scott, W.S. Felps, G.L. Findley and S.P. McGlynn, in preparation.
J.D. Scott and S.P. McGlynn, MCD of non-linear molecules–viewed in a linear molecule basis, *36th Am. Chem. Soc. Northwest Regional Meet., Bozeman, MT, June 17 - 19, 1981.*
27 W.R.S. Garton and F.S. Tompkins, *Astrophys. J., 158* (1969) 839.
28 C.D. Harper and M.D. Levinson, *Opt. Commun., 20* (1977) 107.
29 J.P. Connerade, W.R.S. Garton, M.A. Baig, J. Hormes and S.P. McGlynn, Bonn Synchrotron Center, unpublished data, 1980.
30 J.E. Bayfield, *Phys. Rep., 51* (1979) 317.
31 J.D. Scott and B.R. Russell, *J. Chem. Phys., 63* (1975) 3243.
32 G.C. Causley, J.D. Scott and B.R. Russell, *Rev. Sci. Instrum., 48* (1977) 264.
33 S.P. McGlynn and G.L. Findley, *Proc. Workshop on Far VUV Spectroscopy and Photochemistry, Mülheim a.d. Ruhr, February 24 - 26, 1981,* pp. 99 - 102.
34 M.B. Robin, in M.B. Robin (ed.), *Higher Excited States of Polyatomic Molecules,* Academic Press, New York, 1975.
35 J.W. Lewis, R.V. Nauman, D.B. Bouler and S.P. McGlynn, *J. Am. Chem. Soc.,* in the press.
36 J. Jortner, in E.-E. Koch, R. Haensel and C. Kunz (eds.), *Vacuum Ultraviolet Radiation Physics,* Pergamon, Braunschweig, 1974, p. 263.
37 M. Fox, in A.W. Adamson and P.D. Fleischer (eds.), *Concepts of Inorganic Photochemistry,* Wiley-Interscience, New York, 1975, p. 333.
38 G.L. Findley, J.A. Dagata and S.P. McGlynn, submitted to *Chem. Rev.*